

14. R. A. LaCasse *et al.*, data not shown. Serum was adsorbed sequentially to protein A Sepharose (Sigma) and protein G agarose (Sigma) at 4°C. Adsorption of antibody was confirmed by gp120 ELISA. The solid supports were combined and antibodies were eluted with 100 mM glycine, pH 2.5. The eluate was neutralized and dialyzed by centrifugal ultrafiltration (Microcon-100; Amicon).
15. R. A. LaCasse *et al.*, *J. Virol.* **72**, 2491 (1998).
16. A. Trkola *et al.*, *ibid.*, p. 1876; D. C. Montefiori *et al.*, *ibid.*, p. 3427.
17. K. E. Follis, M. Trahey, R. A. LaCasse, J. H. Nunberg, *ibid.*, p. 7603.
18. Envelope-expressing cultures were incubated with sCD4 [E. A. Berger, T. R. Fuerst, B. Moss, *Proc. Natl. Acad. Sci. U.S.A.* **85**, 2357 (1988)] (5 µg/ml; 1 hour at 37°C) and subsequently washed to remove unbound sCD4. All FI immunogens were fixed with formaldehyde as described in (10).
19. Envelope-defective HIV NL4-3-Luc-R<sup>-</sup>E<sup>-</sup> provirus was pseudotyped with amphotropic MLV envelope protein [H. Deng *et al.*, *Nature* **381**, 661 (1996)].
20. A primary isolate of SIVmac251 [A. L. Langlois *et al.*, *J. Virol.* **72**, 6950 (1998)] was produced in rhesus PBLs.
21. A statistical comparison was performed on data comprising all experimental animals and all virus neutralization assays. A simple model for virus-antibody binding was used to calculate a "binding constant" *K* for each assay, and a mean *K* value was determined for each mouse. Two-sample unpaired *t* tests were performed on log-transformed *K* values to compare groups pairwise. Bonferroni-adjusted comparison demonstrated a significant difference in mean neutralization between FC and FI immunogens (*P* = 0.001). This analysis included 26 independent neutralization assays of FC sera, from all mice receiving FC immunogen, and similarly, 35 assays of FI sera. In all experiments, responses within experimental groups were consistent and uniform.
22. M. P. Cranage *et al.*, *AIDS Res. Hum. Retrovir.* **9**, 13 (1993); P. Putkonen *et al.*, *J. Med. Primatol.* **22**, 100 (1993); L. O. Arthur *et al.*, *Science* **258**, 1935 (1992).
23. Infectious proviruses ACH320.2A.1.2 (320SI) and ACH320.2A.2.1 (320NSI) [M. Groenink *et al.*, *J. Virol.* **65**, 1968 (1991); C. Guillon *et al.*, *AIDS Res. Hum. Retrovir.* **11**, 1537 (1995)] were obtained through the National Institute for Biological Standards and Controls (NIBSC, United Kingdom) AIDS Reagent Program from Hanneke Schuitemaker (Netherlands Red Cross). HIV89.6 [R. Collman *et al.*, *J. Virol.* **66**, 7517 (1992)], SHIV89.6, and SHIV89.6P [K. A. Reimann *et al.*, *ibid.* **70**, 3198 (1996)] were provided with permission by D. Montefiori (Duke University Medical Center). All other primary isolates were obtained through the NIH AIDS Research and Reference Reagent Program and the UNAIDS Network for HIV-1 Isolation and Characterization. PI viruses were subjected to limited expansion in phytohemagglutinin-activated PBLs (2).
24. M. Thali *et al.*, *J. Virol.* **67**, 3978 (1993); N. Sullivan *et al.*, *ibid.* **72**, 4694 (1998).
25. J. M. Gershoni *et al.*, *FASEB J.* **7**, 1185 (1993); S. Lee *et al.*, *J. Virol.* **71**, 6037 (1997).
26. FC vaccine serum (1:10 dilution in cell culture medium) was sequentially adsorbed four times with ~10<sup>6</sup> formaldehyde-fixed COS cells expressing 168P envelope protein. Incubations were for 1 hour at 4°C with rocking. Controls included prebleed serum and formaldehyde-fixed, mock-transfected COS cells. Adsorption of bulk anti-gp120 was monitored by gp120 ELISA. Final sera were tested for neutralization of HIV 168P with U87-CD4-CXCR4 cells. Parallel studies with intact but non-fixed cells yielded concordant results.
27. Pooled FC and FI sera (1:8 dilution) were incubated with attached U87-CD4-CCR5 cells (2 × 10<sup>4</sup> cells per 96-well microculture) for 1 hour at 37°C with occasional mixing. Supernatants were tested for neutralization of HIV 168P with U87-CD4-CCR5 cells.
28. W. Weissenhorn *et al.*, *Nature* **387**, 426 (1997); D. C. Chan, D. Fass, J. M. Berger, P. S. Kim, *Cell* **89**, 263 (1997); W. Weissenhorn, L. J. Calder, S. A. Wharton, J. J. Skehel, D. C. Wiley, *Proc. Natl. Acad. Sci. U.S.A.* **95**, 6032 (1998).
29. C. Wild, T. Oas, C. McDanal, D. Bolognesi, T. Matthews, *Proc. Natl. Acad. Sci. U.S.A.* **89**, 10537 (1992); R. A. Furuta, C. T. Wild, Y. Weng, C. D. Weiss, *Nature Struct. Biol.* **5**, 276 (1998).
30. M. P. D'Souza *et al.*, *J. Infect. Dis.* **175**, 1056 (1997).
31. A. M. Prince *et al.*, *AIDS Res. Hum. Retrovir.* **7**, 971 (1991); E. A. Emmini *et al.*, *Nature* **355**, 728 (1992); A. J. Conley *et al.*, *J. Virol.* **70**, 6751 (1996); M. C. Gauduin *et al.*, *Nature Med.* **3**, 1389 (1997).
32. R. M. Krause, N. J. Dimmock, D. M. Morens, *J. Infect. Dis.* **176**, 549 (1997).
33. J.H.N. was supported by targeted research grant 02560-23-RGV from the American Foundation for AIDS Research (AmFAR), funded in part by Concerned Parents for AIDS Research (CPFA). Additional funds were provided by The University of Montana, NIH AREA grant AI41165, and the M. J. Murdock Charitable Trust. D.R.L. was supported by NIH grant AI33856 and by a grant from AmFAR and is an investigator of the Howard Hughes Medical Institute. We thank E. Walker (Ribi ImmunoChem Research, Incorporated, Hamilton, MT) and L. Griggs for flow cytometry, C. Mackay (Leukosite) and M. Tsang for CCR5 mAbs, W. Ellmeier for the transgenic mouse CCR5 construct, D. Montefiori (Duke University Medical Center) for providing SIVmac251, HIV 89.6, and related SHIV viruses, and C. Weiss (U.S. Food and Drug Administration) for providing amphotropic MLV envelope protein pseudotyped HIV virions. Primary HIV isolates and other reagents were obtained from the NIH AIDS Research and Reference Reagent Program, the NIBSC (UK) AIDS Reagent Program, and the UNAIDS Network for HIV-1 Isolation and Characterization. We are grateful to D. A. Patterson (University of Montana, Department of Mathematics) for statistical analysis of neutralization data, and to J. Moore and D. Montefiori for constructive review of the manuscript. Discussions with C. Barbas III and E. Berger were important in the development of these studies.

13 October 1998; accepted 10 December 1998

## Enhancement of Cation Diffusion Rates Across the 410-Kilometer Discontinuity in Earth's Mantle

S. Chakraborty,\*† R. Knoche, H. Schulze, D. C. Rubie, D. Dobson, N. L. Ross, R. J. Angel

Rates of cation diffusion (magnesium, iron, and nickel) have been determined in olivine and its high-pressure polymorph, wadsleyite, at 9 to 15 gigapascals and 1100° to 1400°C for compositions that are relevant to Earth's mantle. Diffusion in olivine becomes strongly dependent on composition at high pressure. In wadsleyite, diffusion is one to two orders of magnitude faster than in olivine, depending on temperature. Homogenization of mantle heterogeneities (chemical mixing) and mineral transformations involving a magnesium-iron exchange will therefore occur considerably faster in the transition zone than at depths of less than 410 kilometers.

The diffusion of atoms in crystalline solids at high temperature is a process that is controlled by the concentration and mobility of point defects. In Earth's interior, solid state creep (through which mantle convection oc-

curs) and electrical conduction, which is used as a probe of the structure and composition of Earth, are physical processes that depend on diffusion (*I*). The rates of chemical processes (such as the mixing of mantle heterogene-

ities, mineral transformations, and element partitioning during partial melting) are also determined by diffusion rates. Even the sharpness of mantle discontinuities may be controlled by cation diffusion during mantle convection, because the kinetics of phase transformations are likely to be diffusion controlled in such regions (2, 3).

However, diffusion coefficients for high-pressure mantle phases (for example, wadsleyite, ringwoodite, and silicate perovskites) are poorly known because of the difficulties of performing appropriate experiments at the pressures (*P*) and temperatures (*T*) at which these phases are stable (4, 5). Here, we report the diffusion behavior of major elements (Fe

S. Chakraborty, Institut für Mineralogie und Geochemie, Universität zu Köln, Zùlpicher Strasse 49B, 50674 Köln, Germany. R. Knoche, Institut für Mineralogie und Petrographie, Universität Innsbruck, Innrain 52, A-6020, Innsbruck, Austria. H. Schulze, D. C. Rubie, R. J. Angel, Bayerisches Geoinstitut, Universität Bayreuth, 95440 Bayreuth, Germany. D. Dobson and N. L. Ross, Mantle Petrology Group, Department of Geological Sciences, University College London, Gower Street, London WC1E 6BT, UK.

\*To whom correspondence should be addressed. E-mail: Sumit.Chakraborty@rz.ruhr-uni-bochum.de

†Present address: Institut für Mineralogie, Ruhr-Universität Bochum, D-44780 Bochum, Germany.

## REPORTS

and Mg) and a trace element (Ni) in  $(\text{Fe,Mg})_2\text{SiO}_4$  olivine and wadsleyite at  $P$ - $T$  conditions in the vicinity of the olivine-wadsleyite phase boundary, which marks the upper boundary of the mantle transition zone. We use starting compositions of  $X_{\text{Mg}} = \text{Mg}/(\text{Mg} + \text{Fe}) = 0.8$  to 1.0, which are relevant for Earth's mantle.

High-pressure experiments were performed on diffusion couples that consisted of two single crystals (olivine) and a single crys-

tal plus a coarse-grained polycrystal (wadsleyite) (6). Each diffusion couple (0.2 to 0.5 mm in length) was inserted in a thick-walled Au capsule that was contained in a multianvil octahedral pressure cell (Fig. 1) (7). The experiments were performed with a 1000-metric ton multianvil apparatus at conditions of 9 to 15 GPa and 1100° to 1400°C for times up to 24 hours (Table 1) (8). The oxygen fugacity ( $f_{\text{O}_2}$ ) during the experiments was estimated to be  $10^{-8}$  to  $10^{-9}$  bars (9). After

quenching and decompression, the samples were sectioned perpendicular to the diffusion interface, examined by optical microscopy, and studied with an electron microprobe (10, 11).

In the case of wadsleyite, for which the compositional range is narrow ( $X_{\text{Mg}} = 0.82$  to 0.90), simple equations for diffusion in semi-infinite media could be fit to normalized concentration profiles (Fig. 2A) to obtain compositionally independent diffusion coefficients (11). At 15 GPa, we obtained diffusion coefficients of  $7 (\pm 1) \times 10^{-15}$  m<sup>2</sup>/s at 1200°C and  $3 (\pm 1) \times 10^{-15}$  m<sup>2</sup>/s at 1100°C (Table 1). These results give an estimate for the activation energy of 145 kJ/mol (compared to 226 kJ/mol, which was obtained for olivine at 1 bar) (12).

The concentration profiles from the olivine samples (Fig. 2A) are much shorter than the wadsleyite profiles, even though the olivine diffusion anneals were performed at a considerably higher temperature (Table 1). The profiles therefore demonstrate that the diffusion of these cations in wadsleyite is much faster than it is in olivine. In addition, the diffusion behavior in olivine at 9 to 12 GPa is qualitatively different from that in wadsleyite, as well as in olivine at lower pressures. In contrast to compositional profiles from diffusion experiments on similar olivine crystals at 1 bar (12), the profiles from all high-pressure experiments (9 to 12 GPa at 1400°C) are strongly asymmetric (Fig. 2A), indicating that the Fe-Mg diffusion coefficient is strongly dependent on composition at high pressure. Because of this dependence, it was not possible to fit a simple diffusion equation to the profiles, and instead, we per-

**Fig. 1.** (A) Reflected-light optical micrograph of a section through the central part of the high-pressure cell after a diffusion experiment at 15 GPa and 1200°C for 24 hours (H654). The wadsleyite sample can be seen at the center of the Au capsule, 0.5 mm from the thermocouple junction. Scale bar, 1 mm. (B) Backscattered electron image showing details of the sample. The interface between the two halves of the diffusion couple is indicated by arrows; the grain boundaries in the polycrystalline part are clearly visible. The position of one of the measured compositional profiles is indicated by a dashed line; this direction corresponds to [010] of the single crystal. The absence of a change in contrast across the sample is the consequence of the small compositional range across the diffusion couple. Scale bar, 100  $\mu\text{m}$ .

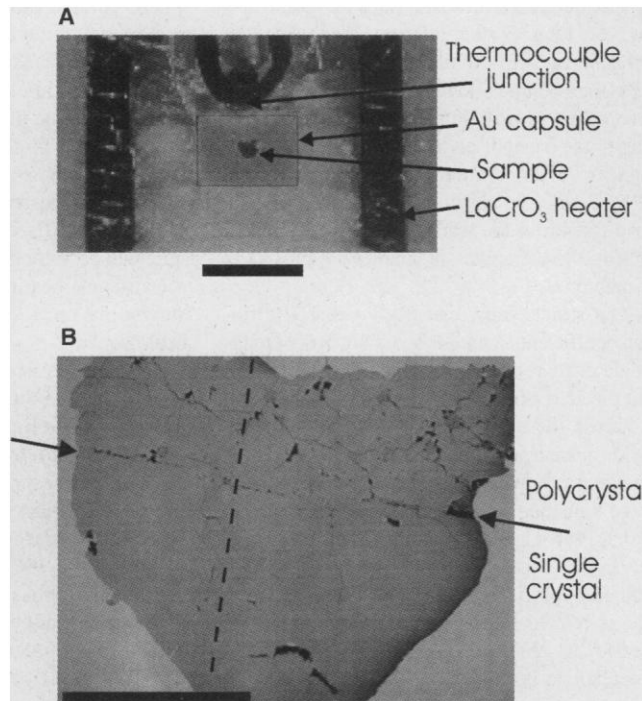
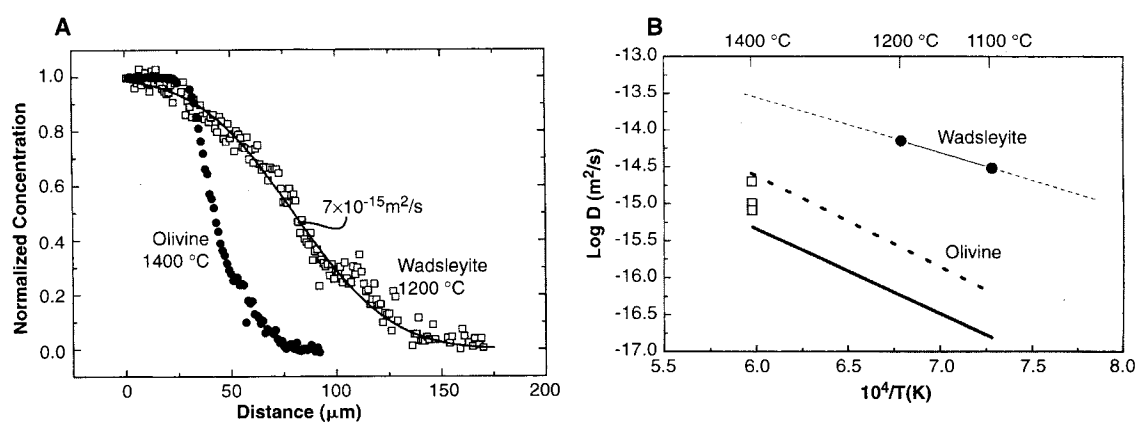


**Fig. 2.** (A) Normalized Mg-Fe concentration profile in wadsleyite at 1200°C and 15 GPa for 24 hours (run H654) (open squares) and best fit to the data (solid line). The normalized concentration  $C' = (C_1 - C_x)/(C_1 - C_2)$ , where  $C_i = X_{\text{Mg}}/(X_{\text{Mg}} + X_{\text{Fe}})$ ,  $C_1$  and  $C_2$  are the starting compositions of the diffusion couple, and  $C_x$  is the measured composition at distance  $x$ . The profile spans a small compositional range ( $X_{\text{Mg}} = 0.82$  to 0.90), which accounts for the scatter in the data. A normalized Mg-Fe concentration profile in olivine at 1400°C and 9 GPa for 24 hours (run H776) (solid circles) is also shown ( $C_1 = 0.82$  and  $C_2 = 1.0$ ) and is much shorter than the wadsleyite profile, despite the higher temperature. (B) Summary of Mg-Fe interdiffusion results for olivine and wadsleyite. Squares represent olivine ( $X_{\text{Mg}} = 0.86$ ); data at 9, 11, and 12 GPa (1400°C) are from this study. The thick solid line represents diffusion along [001] at  $f_{\text{O}_2} = 10^{-12}$  bar, based on measurements carried out at 1 bar (12). The thick dashed line is based on the same data that were corrected for  $f_{\text{O}_2}$  (to  $10^{-8}$  bar) (13). Our data



reinforce the weak pressure dependence of diffusion rates in olivine. Circles represent diffusivities in wadsleyite that were measured at 1100° and 1200°C at a mean composition of  $X_{\text{Mg}} = 0.86$ , with the thin dashed line showing an approximate extrapolation to higher and lower temperatures. The error bars that were obtained from a statistical fit of compositional profiles are on the order of the size of the symbols. Diffusivities in wadsleyite are higher than the measured values in olivine at higher temperatures, and for any reasonable positive value of activation energy, diffusion rates in wadsleyite will be faster than those in olivine with the same composition over a wide range of temperature.

formed a Boltzman-Matano analysis [see (12) for details].

Compositional profiles for the trace element Ni show that diffusion coefficients for this element are similar to those for Fe-Mg interdiffusion. Nickel diffusion is much faster in wadsleyite than in olivine and also depends strongly on the composition ( $X_{Mg}$ ) of the latter phase. Only in some cases (for example, for Mg-rich olivine at 9 GPa) is Ni diffusion slightly slower than Mg-Fe interdiffusion, but only by a factor of 2. Thus, the diffusion behavior documented above is not only specific to Fe-Mg exchange but is also valid for the transport of other cations.

Our Mg-Fe diffusion coefficients for olivine at high pressure are similar to the values that were previously obtained at 1 bar (12). Because oxygen fugacity is uncertain at high pressure (9), we compared the high-pressure results that were obtained for diffusion at 1400°C with 1-bar diffusivities that were (i) measured experimentally at  $f_{O_2} = 10^{-12}$  bars and (ii) estimated at  $f_{O_2} = 10^{-8}$  bars by extrapolation (13). The small pressure dependence of diffusivity is consistent with other studies that have shown that the activation volumes for Mg-Fe interdiffusion and Mg tracer diffusion in olivine are small ( $<3.5$  cm<sup>3</sup>/mol) (4). However, high pressure has a substantial effect on the compositional dependence of diffusion rates in olivine. Diffusion coefficients change by about an order of magnitude in the range  $X_{Mg} = 0.86$  to 0.98 at 12 GPa and 1400°C (Table 1). In contrast, at 1 bar, the diffusion coefficients change only by a factor of 2 over the same compositional range (12). The general trend at all pressures is that the diffusion rates increase as the composition becomes richer in the Fe<sub>2</sub>SiO<sub>4</sub> component. The cause of the strong compositional dependence at high pressure may be that diffusion is more sensitive to changes in the environment of a cation when the structure is in a compressed state. Similarly, diffusion rates of large cations (Fe and Ca) in garnet show a stronger dependence on composition than

small cations (Mg) at a fixed pressure (14).

The diffusion coefficients obtained in olivine for a mean composition of  $X_{Mg} = 0.86$  at 9 to 12 GPa are smaller than those obtained for wadsleyite of similar composition (Fig. 2B), despite the lower temperatures (1100° to 1200°C) and higher pressures (15 GPa) at which the wadsleyite samples were annealed. Given the small pressure dependence of diffusivity in olivine that is found in this and other studies (4), it is meaningful to compare diffusivities in wadsleyite obtained here with the large database for diffusion rates in olivine at 1 bar. At 1100°C, the difference between the diffusion rates in olivine and wadsleyite at 15 GPa (for a composition of  $X_{Mg} = 0.86$ ) is about two orders of magnitude (Fig. 2B); the exact magnitude depends on the pressure and oxygen fugacity. When normalized to a temperature of 1400°C with the preliminary activation energy for diffusion in the wadsleyite obtained at 145 kJ/mol, the difference is smaller (~1.5 orders of magnitude).

Our results show that Mg-Fe and Ni diffusion coefficients increase by two orders of magnitude or more (depending on temperature) and that the activation energy substantially decreases across the olivine-wadsleyite phase boundary. Similar changes were recently reported for electrical conductivity across the olivine-wadsleyite transition for a similar composition ( $X_{Mg} = 0.9$ ) (15). The enhancement of transport rates across the phase boundary can be partly explained by an increased vacancy concentration that is related to the higher Fe<sup>3+</sup> content of wadsleyite (16). In addition, the mobility of point defects is likely to be higher in wadsleyite than in olivine because the jump distances between neighboring octahedral sites are shorter (17). Because of the structural similarities between wadsleyite and its higher pressure polymorph (ringwoodite), cation diffusion might also be fast in the latter phase (18).

Thus, rates of processes that are controlled by the diffusion of cations such as Mg, Fe, and Ni should be at least an order of magnitude

faster in the transition zone (410 to 660 km depth and  $T = 1500^\circ$  to  $1600^\circ\text{C}$ ) than at shallower depths in the upper mantle (19). Such processes include the homogenization of chemical heterogeneities that are introduced into the mantle by the subduction of sediments and oceanic lithosphere (20). In subducting slabs, where temperatures are relatively low, the enhancement in homogenization rates should be even greater because of the relatively low activation energy for diffusion in wadsleyite. For example, in a coarse-grained mantle at 1400°C, where volume diffusion dominates, the diffusive-mixing time scale (given by  $x^2/D \sim t$ , where  $x$  is distance,  $D$  is the diffusion coefficient and  $t$  is time) for homogenizing a heterogeneous volume that is ~1 m in radius is ~50 million years in the olivine-bearing part and only ~1 million years once olivine is transformed to wadsleyite. In a colder mantle at 1100°C, the difference is more drastic; the volume will be homogenized in 10 million years in a wadsleyite-bearing mantle, whereas it would survive for up to 2 billion years in the olivine-bearing part.

The results from this study may have implications for other transport processes (such as creep and electrical conduction) that are also controlled by point defects (21). In a model of the response of the olivine-wadsleyite phase boundary to convective flow across the 410-km discontinuity, it was previously assumed that Mg-Fe diffusion rates are the same in both phases (2). Our new data imply that, for this model, the 410-km discontinuity should be thinner in regions of upwelling than in regions of downwelling.

References and Notes

1. D. L. Kohlstedt, B. Evans, S. J. Mackwell, *J. Geophys. Res.* **100**, 17587 (1995); S. Constable and A. Duba, *ibid.* **95**, 6967 (1990).
2. V. S. Solomatov and D. J. Stevenson, *Earth Planet. Sci. Lett.* **125**, 267 (1994).
3. C. R. Bina and M. Kumazawa, *Phys. Earth Planet. Int.* **76**, 329 (1993).
4. Diffusion in low-pressure phases of Earth's upper mantle, such as olivine and garnet, has been studied extensively at 1 bar. A few studies have also been performed at high pressure for both tracer diffusion and chemical diffusion [S. Chakraborty and J. Ganguly, *Contrib. Mineral. Petrol.* **111**, 74 (1992); S. Chakraborty, J. R. Farver, R. A. Yund, D. C. Rubie, *Phys. Chem. Miner.* **21**, 489 (1994); O. Jaoul, Y. Bertran-Alvarez, R. C. Liebermann, G. D. Price, *Phys. Earth Planet. Inter.* **89**, 199 (1995); S. Chakraborty and D. C. Rubie, *Contrib. Mineral. Petrol.* **122**, 406 (1996)].
5. In a previous study of diffusion in high-pressure polymorphs of olivine [ $\beta$  and  $\gamma$  phases of (Mg,Ni)<sub>2</sub>SiO<sub>4</sub>], it was concluded that Mg-Ni interdiffusion is three orders of magnitude faster in the high-pressure polymorphs (wadsleyite and ringwoodite structures) than in  $\alpha$  phase (olivine structure) (22). However, interpretation of these results is complicated because of the simultaneous occurrence of polymorphic phase transformations and diffusion in the experiments. In addition, results from (Mg,Ni)<sub>2</sub>SiO<sub>4</sub> compositions may not be good indicators for diffusion behavior in Fe-bearing mantle compositions.
6. The olivine diffusion experiments were performed on pairs of oriented cylinders (which had a length of 200  $\mu\text{m}$  and a diameter of 200 to 250  $\mu\text{m}$ ) that were prepared from single crystals of (i) synthetic forsterite

**Table 1.** Conditions and results of high-pressure diffusion experiments. For the olivine samples, formally propagated errors on results from Boltzman-Matano analysis are ~25%; real errors are likely to be higher. Nickel diffusion coefficients are similar to the  $D_{Mg-Fe}$  values and are therefore not reported separately.

Run	P (GPa)	T (°C)	Time (hours)	Composition ( $X_{Mg}$ )	$D_{Mg-Fe}$ (m <sup>2</sup> /s)
<i>Wadsleyite</i>					
H654	15	1200	24	0.82–0.90	$7 (\pm 1) \times 10^{-15}$
H696	15	1100	15	0.82–0.90	$3 (\pm 1) \times 10^{-15}$
<i>Olivine</i>					
H776	9	1400	24	0.86	$1 \times 10^{-15}$
				0.92	$5 \times 10^{-16}$
				0.98	$3 \times 10^{-16}$
H777	11	1400	24	0.86	$2 \times 10^{-15}$
				0.92	$1 \times 10^{-15}$
				0.98	$4 \times 10^{-16}$
H778	12	1400	24	0.86	$8 \times 10^{-16}$
				0.92	$3 \times 10^{-16}$
				0.98	$3 \times 10^{-17}$

ite ( $X_{Mg} = 1.0$ ) and (ii) an unusually Fe-rich ( $X_{Mg} = 0.82$ ) Ni-bearing [ $\sim 3000$  parts per million (ppm)] San Carlos olivine (12). For the wadsleyite diffusion experiments, we synthesized two samples of wadsleyite in multianvil experiments and characterized them by optical microscopy, x-ray diffraction, and electron microprobe analysis. In one case, single crystals of olivine ( $X_{Mg} \approx 0.9$  and  $\sim 3000$  ppm of Ni) from the Troodos ophiolite complex in Cyprus were transformed to wadsleyite of the same composition at 15 GPa and 1250°C; crystals in the form of (010) plates, with dimensions of 150 to 220  $\mu\text{m}$  and containing occasional (010) twins, were obtained. The second sample was synthesized by transforming synthetic olivine powder ( $X_{Mg} \approx 0.82$  and  $< 100$  ppm of Ni) at 16 GPa and 1800°C to polycrystalline wadsleyite with an average grain size of 60 to 100  $\mu\text{m}$ .

- The crystals were prepared for diffusion experiments by polishing surfaces (which were approximately perpendicular to [010], in the case of the single crystals) with a diamond polishing compound (0.25- $\mu\text{m}$  grit size). Gold was used as the sample container because it is mechanically weak and prevents the crystals from being stressed or damaged during pressurization; also, unlike Pt, Au does not react chemically with the sample to cause a loss of Fe. The sample container was prepared by drilling a 250- $\mu\text{m}$ -diameter hole in a Au wire that is 1 mm in diameter; the samples were placed together in this hole with the polished surfaces in contact. The capsule was closed by deforming the Au to obtain a cylinder with a length of 1 mm and a diameter of 1 mm, with the sample located at the center.
- In the multianvil experiments [R. C. Liebermann and Y. Wang, in *High-Pressure Research: Applications to Earth and Planetary Sciences*, vol. 67 of *Geophysical Monograph Series*, Y. Syono and M. H. Manghnani, Eds. (American Geophysical Union, Washington, DC, 1992), pp. 19–31] a MgO octahedron with a 14-mm edge length was used as the pressure cell. A cylindrical LaCrO<sub>3</sub> heater with a stepped wall thickness was used to minimize thermal gradients. Temperature was measured with an axially located W3%Re/W25%Re thermocouple and was controlled to  $\pm 1^\circ\text{C}$  during experiments that had durations of up to 24 hours. High pressure was generated using eight 32-mm cubic WC anvils with corners truncated to an edge length of 8 mm. Pressure was calibrated at 1000°C using phase transformations in SiO<sub>2</sub>, Fe<sub>2</sub>SiO<sub>4</sub>, and Mg<sub>2</sub>SiO<sub>4</sub> with an uncertainty of 0.5 GPa. After pressurization, temperature was raised to the desired value at a rate of 100°C/min; after the diffusion anneal, samples were quenched to  $< 300^\circ\text{C}$  in  $\sim 1$  s. Because the distance between the thermocouple and sample was  $\sim 0.5$  mm (Fig. 1), temperature errors due to thermal gradients are likely to be  $< 20^\circ\text{C}$ . [For further details, see D. C. Rubie, C. R. Ross, M. R. Carroll, S. C. Elphick, *Am. Mineral.* **78**, 574 (1993), and D. C. Rubie, S. Karato, H. Yan, H. St. C. O'Neill, *Phys. Chem. Miner.* **20**, 315 (1993).]
- Oxygen fugacity is estimated by assuming that the Au capsule maintained a closed system and that the volume change of the samples on compression was negligible. Given the volume and composition of olivine, the free energy of the system is minimized to obtain the equilibrium oxygen fugacity [see R. Dohmen, S. Chakraborty, H. Palme, W. Rammensee, *Am. Mineral.* **83**, 970 (1998) for details]. Calculations with published thermodynamic data [R. A. Robie, B. S. Hemingway, J. R. Fisher, *U.S. Geol. Surv. Bull.* **1452** (1979); D. R. Sull and H. Prophet, Eds., *JANAF Thermochemical Tables* (Government Printing Office, Washington, DC, ed. 3, 1971)] yield  $f_{O_2} = 10^{-8}$  to  $10^{-9}$  bars, which is about an order of magnitude lower than that of the wüstite-magnetite buffer at 1400°C and 15 GPa. Uncertainties in this estimate are mainly of consequence when comparing results of this study with data from previous studies at 1 bar (Fig. 2B).
- Analyses were performed with Cameca SX-50 (Bayreuth) and JEOL 8900 RL (Köln) electron microprobes. Standards were silicates and oxides, and beam conditions were 15 kV and 15 nA with counting times of 20 s.
- For the polycrystalline wadsleyite, detailed element mapping was performed to define the boundary conditions under which diffusion occurred. Results show that

contributions from grain boundary diffusion in the polycrystalline material (Fig. 1) can be neglected in the 1100°C experiment, and the diffusion process was therefore treated as volume diffusion between two initially homogeneous slabs. The appropriate solution to the diffusion equation [for example, J. Crank, *The Mathematics of Diffusion* (Oxford Univ. Press, Oxford, 1975), Eq. 2.14] was fit to the concentration profiles to determine the diffusion coefficient. In the experiment at 1200°C, grain boundary diffusion in the somewhat finer grained polycrystalline material contributed substantially to the diffusion process. In this case, a solution was used with a boundary condition that corresponded to a constant composition at the surface of the single crystal, as seen in the elemental concentration maps [J. Crank, *The Mathematics of Diffusion* (Oxford Univ. Press, Oxford, 1975), Eq. 3.13]. The difference in behavior of the two samples is related to the slight difference in grain size rather than to the temperature at which the samples were annealed. The solution for the single-crystal part is the same, irrespective of which equation is used to fit the data.

- S. Chakraborty, *J. Geophys. Res.* **102**, 12317 (1997).
- Diffusion rates at  $f_{O_2} = 10^{-8}$  bar were calculated with the measured dependency of diffusion rates on oxygen fugacity ( $D \propto f_{O_2}^{1/6}$ ) as reported by D. K. Buening and P. R. Buseck, *ibid.* **78**, 6852 (1973), and A. Nakamura and H. Schmalzried, *Ber. Bunsenges. Phys. Chem.* **88**, 140 (1984). Recent unpublished data from our laboratory are consistent with the dependencies found by these authors.
- S. Chakraborty and J. Ganguly, *Contrib. Mineral. Petrol.*

- 111, 74 (1992); J. Ganguly, W. Cheng, S. Chakraborty, *ibid.* **131**, 171 (1998).
- Y. Xu, B. T. Poe, T. J. Shankland, D. C. Rubie, *Science* **280**, 1415 (1998).
- Measured Fe<sup>3+</sup> contents of wadsleyite are typically 0.03 to 0.04 weight % as opposed to  $< 0.01$  weight % in olivine when total Fe contents are similar (23).
- The shortest Mg-Mg distances in Mg<sub>2</sub>SiO<sub>4</sub> olivine are 2.99 Å [K. Fujino, S. Sasaki, Y. Takeuchi, R. Sadanaga, *Acta Crystallogr.* **B37**, 513 (1981)], whereas in wadsleyite, there are many distances between 2.80 and 3.06 Å [H. Horiuchi and H. Sawamoto, *Am. Mineral.* **66**, 568 (1981)].
- The electrical conductivities of wadsleyite and ringwoodite are almost identical (15), and these phases also have similar Fe<sup>3+</sup> contents (23).
- A similar conclusion was reached by Farber *et al.*, but they probably overestimated the effect by two orders of magnitude (22).
- L. H. Kellogg and D. L. Turcotte, *J. Geophys. Res.* **95**, 421 (1990).
- S. J. Mackwell, D. Dimos, D. L. Kohlstedt, *Philos. Mag. A* **57**, 779 (1988); B. J. Wanamaker, *Geophys. Res. Lett.* **21**, 21 (1994).
- D. L. Farber, Q. Williams, F. J. Ryerson, *Nature* **371**, 693 (1994).
- H. St. C. O'Neill *et al.*, *Am. Mineral.* **78**, 456 (1993).
- This research was partly supported by the European Union's TMR—Large Scale Facilities Programme (contract ERBFMGECT980111) and the Natural Environment Research Council (grant NERC GR9/03066).
- 21 September 1998; accepted 18 November 1998

## Phytoplankton Community Structure and the Drawdown of Nutrients and CO<sub>2</sub> in the Southern Ocean

Kevin R. Arrigo,\* Dale H. Robinson, Denise L. Worthen, Robert B. Dunbar, Giacomo R. DiTullio, Michael VanWoert, Michael P. Lizotte

Data from recent oceanographic cruises show that phytoplankton community structure in the Ross Sea is related to mixed layer depth. Diatoms dominate in highly stratified waters, whereas *Phaeocystis antarctica* assemblages dominate where waters are more deeply mixed. The drawdown of both carbon dioxide (CO<sub>2</sub>) and nitrate per mole of phosphate and the rate of new production by diatoms are much lower than that measured for *P. antarctica*. Consequently, the capacity of the biological community to draw down atmospheric CO<sub>2</sub> and transport it to the deep ocean could diminish dramatically if predicted increases in upper ocean stratification due to climate warming should occur.

Climate models (1) indicate that over the next half century, the Southern Ocean carbon (C) cycle will change dramatically in response to rising atmospheric CO<sub>2</sub>. Increased precipitation is predicted to intensify surface ocean stratification, thereby decreasing the downward flux of C and reducing the capacity of the Southern Ocean to take up anthropogenic CO<sub>2</sub>. The biological response to the predicted changes in ocean dynamics is poorly understood. Here we present results from the oceanographic program Research on Ocean-Atmosphere Variability and Ecosystem Response in the Ross Sea (ROAVERRS), cruise

NBP96-6 (2), that show how increased stratification in the Ross Sea would affect phytoplankton community structure and CO<sub>2</sub> and nutrient drawdown in the Ross Sea.

Three spatially distinct phytoplankton assemblages (3) dominated the the Ross Sea during 1996–97, with phytoplankton community structure varying as a function of the depth of the mixed layer. The assemblage with the widest distribution and highest biomass of chlorophyll a (Fig. 1A) was dominated by *Phaeocystis antarctica* and extended from the Ross Ice Shelf northward to 75°S (Fig. 1B). Mixed layers in the *P. antarctica*–